

# COMPACT MARX GENERATORS FOR THE GENERATION OF HIGH POWER MICROWAVES

J. R. Mayes, W. J. Carey, W. C. Nunnally,<sup>1</sup> L. Altgilbers,<sup>2</sup> M. Kristiansen<sup>3</sup>

*Applied Physical Electronics, L.C.*

*Austin, Texas 78734*

## Abstract

Traditional Marx generators have been primarily reserved for energy storage and pulse-charging sources. However, recent work<sup>4</sup> has demonstrated the Marx generator's effectiveness in delivering ultra-short impulses at very intense power levels. This paper discusses two very compact Marx generators capable of delivering voltage pulses of several hundred kV, durations of several nano-seconds to 10's of nanoseconds, and risetimes as fast as 200 ps. Performance of these generators will be discussed as well as radiation results with the generator directly driving a TEM horn antenna. Further discussion will be made toward the application of the Marx generator driving various microwave devices including the Backward Wave Oscillator.

## I. INTRODUCTION

Applied Physical Electronics, L.C., or APELC, has successfully developed Marx generators with impulses well suited for the direct generation of Ultra Wideband (UWB) signals as well as for driving narrowband microwave devices such as the Backward Wave Oscillator (BWO). Ideally, UWB sources require extreme voltage pulses that have risetimes of only a few hundred picoseconds and pulse widths of up to several nanoseconds. Conversely, narrowband sources require longer, more energetic pulses of similar power levels.

This paper presents two generators for both the UWB and narrowband applications. Each generator is presented for basic performance parameters. Applications of each source are then presented.

## II. BACKGROUND

### A. The Wave Erection Marx Generator

The most efficient, compact and economical method of generating a repetitive, large magnitude, electromagnetic impulse is the wave erection of a spark gap-switched Marx circuit. Wave erection is necessary

to obtain the fast voltage risetimes from the Marx circuit that generates the ultra-wideband of frequencies necessary for high-resolution radar or the interdiction of flight controls and computer memories for electronic warfare.

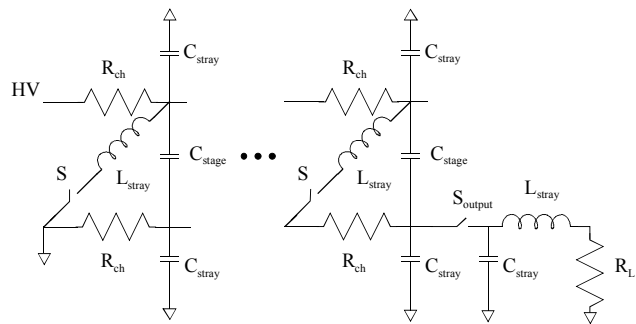


Figure 1. The Wave-Erection Marx Generator.

The conventional Marx circuit, illustrated in Figure 1, charges capacitors in parallel through resistors, and then switches the capacitors, using spark gap switches, in series to add the individual capacitor voltages at the output terminals. This approach multiplies the charge voltage by the number of stages to yield a large output voltage. Proper design of the stray capacitance and the inter-stage capacitance, in concert with coupling the spark gaps via ultra-violet energy, results in a sub-ns risetime for output voltages of several hundred kV at moderate per pulse energies.

### B. APELC's Ultra-Wideband Generator

APELC's impulse generators are based on very compact geometries, delivering low amounts of energy in just a few nanoseconds. These generators may be battery-powered for autonomous applications.

The generator used for this discussion was a 17-stage Marx with a 30 kV charging voltage. As shown in Figure 2, the generator delivers a short impulse that is approximately 1 ns, full width half maximum (FWHM), with a risetime of 200 ps and a voltage efficiency of 65%. The impulse peaks at about 360 kV and is followed by a longer plateau of approximately 125 kV, which decays to zero within 14 ns. The peak power of the impulse is approximately 2.6 GW.

This effort was supported by BMDO under U.S. Army contract number DASG60-99-M-0051

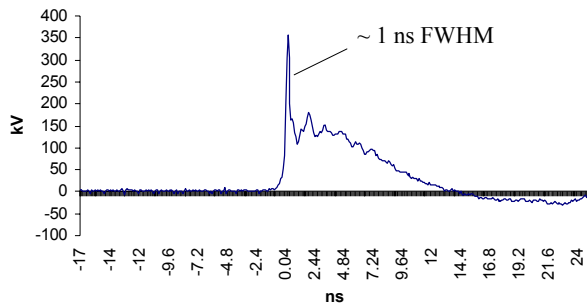


Figure 2. A typical output pulse from the impulse Marx generator.

Physically, this generator is encased in a 76 mm diameter tube of length of 1 m. At approximately, 15 lb, this generator is well suited as a man portable system.

### C. APELC's Narrowband Source Generator

APELC's narrowband source generator is also based on the wave-erection principle. This generator is a 13-stage design sourced by a 40 kV supply voltage. The Marx circuit occupies approximately 60% of the cylindrical housing structure (127 mm diameter, 1 m length), allowing additional volume for future circuitry

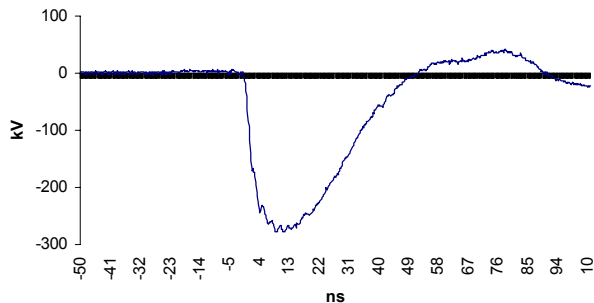


Figure 3. A typical output pulse from the narrowband generator source.

As shown in Figure 3, the output waveform is characterized by a 3 ns risetime and a peak voltage of 270 kV, or 1.5 GW into the 50 Ohm load, and delivers 32 J in approximately 20 ns, FWHM.

## III. APPLICATIONS

### A. Low Jitter Operation for Pulse Synchronization

Low temporal jitter of the impulse Marx generator may be required for multi-source applications or timing applications.<sup>5</sup> For the Marx generator to be a viable candidate for phased array systems, the jitter must be reduced to a small fraction of its pulse width, 200 ps in these case of the 1 ns impulse. Similar results must also be achieved for multiple pulse addition circuits such as Gatling-styled systems and bistatic radar systems.

There are three basic triggered spark gap types including the trigatron, the laser-triggered, and the field distortion.<sup>6</sup> The trigatron gap is a three electrode gap with the voltage held off between the anode and cathode. The third electrode, or the trigger pin, is placed within the cathode electrode such that initial closure of the spark gap begins with a breakdown between the trigger pin and the cathode. This initial breakdown generates a plasma in the high field region between the anode and cathode and ultimately leads to the breakdown of the main gap. These systems are very easily fabricated and simply require a high voltage pulse for triggering. Unfortunately, these systems result in high jitter values due to the fact that two breakdown events are required for switch closure.

The laser-triggered spark gap relies on optical energy to vaporize a portion of the metal electrode. The hot metal vapor emits ultraviolet energy, which then produces free electrons at the electrode surface. Furthermore, the laser also pre-ionizes the path back to the opposite electrode. The electric field then heats the streamer to reduce the resistance and leads to closure of the spark gap. These systems are more difficult to fabricate and require large pulsed laser systems for triggering. However, the lowest spark gap jitter recorded came from a laser-triggered spark gap and resulted in a jitter of 50 ps.

The third spark gap-triggering method, the field distortion gap, a dc-biased pin is placed between the anode and cathode such that the electric field is not disturbed. Gap closure is initiated when a negative pulse is delivered to the trigger pin and results in a highly distorted electric field between the main electrodes. The field distortion spark gap is ideal for low jitter applications, since the two breakdown events occur simultaneously.

The closure of a spark gap is a statistical process. However, the breakdown process is sequential. Consider a spark gap that is closed by over-volting. Initially, the spark gap voltage is set just below the statistical breakdown level,  $V_{SB}$ . The time for the breakdown process to occur is dependent on four events: (1) the statistical time delay for the appearance of a free electron,  $t_{sd}$ , which may be reduced to zero with the application of a UV source; (2) the streamer formation time,  $t_{sf}$ , which is inversely proportion to the electric field; (3) the channel heating time,  $t_{ch}$ , which is also inversely proportional to the electric field; and (4), the trigger pulse risetime,  $t_r$ .

Reduction in temporal jitter for the field distortion gap is primarily dependent on three parameters, UV illumination, a fast-rising trigger pulse (10 kV/ns), and a trigger voltage approximately equal in magnitude to the charging voltage. Achieving a spark gap jitter of less than 200 ps will require an extremely fast trigger source.

The method chosen for triggering the field distortion spark gap uses a short coaxial line, as illustrated in Figure 4. This coaxial line, referred to as the trigger line, is DC biased to  $\frac{1}{2}$  the charging voltage of the spark gap. Note that the trigger switch must hold off the DC bias voltage.

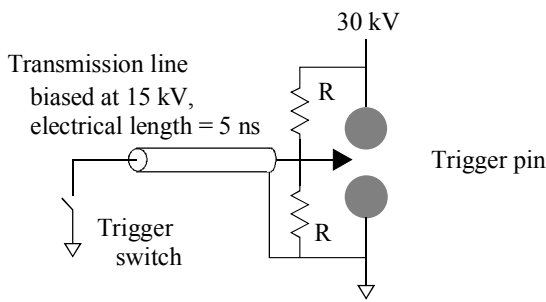


Figure 4. Triggering the field distortion gap.

Upon closure of the trigger switch, a reflected pulse of  $-\frac{1}{2}$  the spark gap-charge voltage and of a length that is twice that of the charged transmission line propagates toward the spark gap, as shown in Figure 5. Arriving at the end of the trigger pin, the pulse doubles in magnitude, resulting in a potential of minus one-half the charge voltage. This results in a highly distorted field between the electrodes due to the presence of the sharp pin at the negative potential.

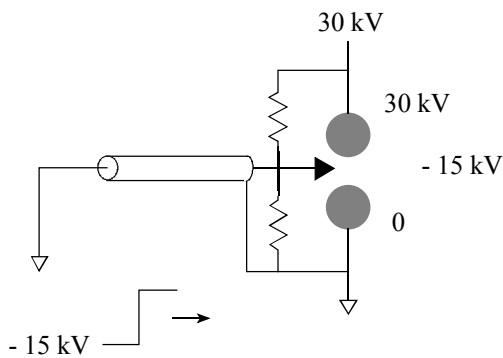


Figure 5. Transient-wave propagation in the field distortion gap.

Experimentally, the jitter performance is measured using the three Marx generator system described by Figure 6. Each generator is connected to a common trigger circuit, which is a krytron-based circuit designed to hold off 15 kV. Likewise, each generator is connected to a single output transmission line. To temporally separate the individual pulses, the trigger lines connecting each generator to the trigger circuit are each unique in length.

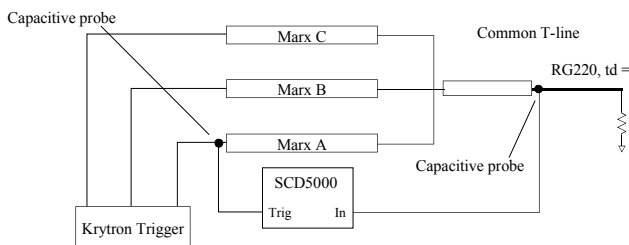


Figure 6. Experimental arrangement for jitter measurements.

Two capacitive voltage dividers were used to measure the generators' performances. The first probe, located at the trigger input of Marx A and was used to trigger the SCD5000, and thus becomes the jitter reference point. The second probe was located on the output transmission line and is connected to the input of the SCD5000.

The samples of the Figure 7, for Marx A, result from a trigger line with a length of 5 ns. The spread of the waveforms was 540 ps, with a standard deviation of 114 ps. The trigger line between Marx B and the krytron trigger circuit was set to an electrical length of 30 ns. The resulting set of waveforms, shown in Figure 8 show an increase in rms jitter, approximately 196 ps, and a spread of 620 ps. Finally, the trigger line length for Marx C was chosen at 60 ns. Figure 9 reveals the sample waveforms. The spread was approximately 1.18 ns, with a jitter of 285 ps. The effect of dispersion become obvious from these measurements.

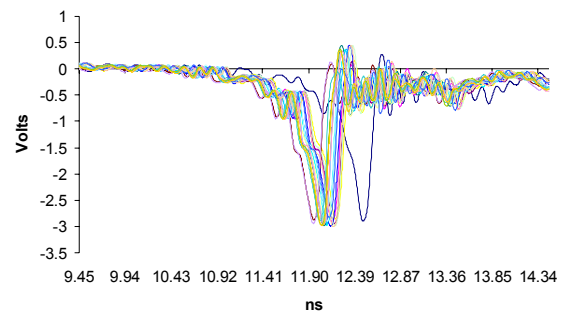


Figure 7. Output samples with a 5 ns trigger line.

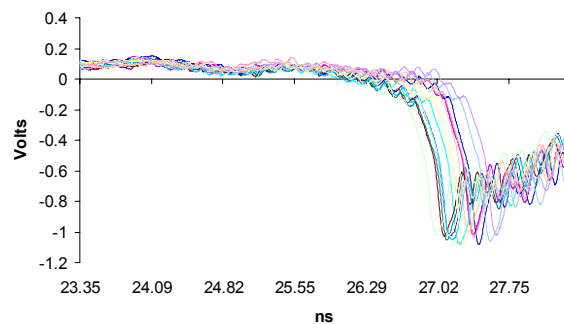


Figure 8. Output samples with a 30 ns trigger line.

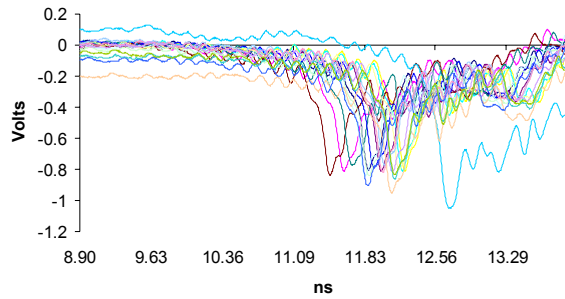


Figure 9. Output samples with a 60 ns trigger line.

### B. Generation of UWB Signals

The impulse Marx generator was tested for its ability to directly generate microwave energy in the form of an UWB signal. As shown in Figure 10, the Marx generator directly drives a rudimentary TEM horn antenna. Approximately 100 m from the source, an EMCO 3106 antenna was used for radiative measurements. Additional measurements were made with a crystal detector.

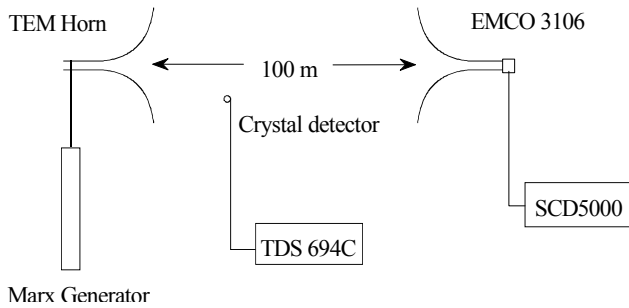


Figure 10. Test range setup for UWB measurements.

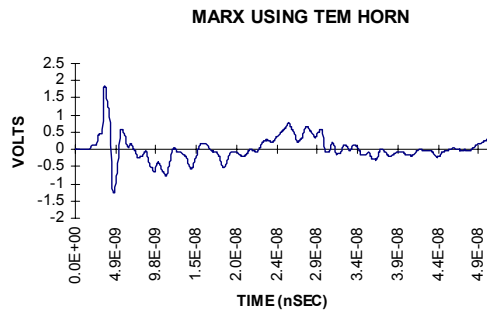


Figure 11. Waveform measurement of a Marx generator driving a TEM horn and measured with an EMCO 3106 antenna.

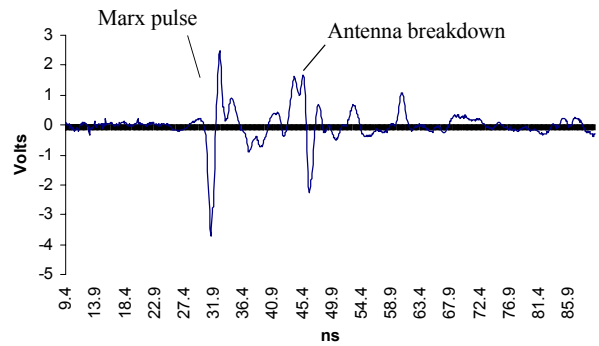


Figure 12. Waveform measurement of a Marx generator driving a TEM horn and measured with an uncalibrated crystal detector.

The Waveform of Figure 11 reveals the radiative results from the Marx-based system. The generator was operated such that it only delivered a 125 kV pulse, thus minimizing the breakdown problems. Subsequent measurements were made with an uncalibrated crystal detector, as shown in Figure 12. Field strength measurements were not made.

### C. Single Pulse Systems with a BWO

The narrowband Marx generator was used to drive the cathode of a Russian-made BWO in a collaborative effort with Texas Tech University<sup>3</sup>. As shown in Figure 13, the Marx generator directly drove the cathode and was temporally aligned with the magnetic field pulse. An uncalibrated, integrated B-dot probe was used to monitor the generated signal, as well as a fluorescent witness plate.

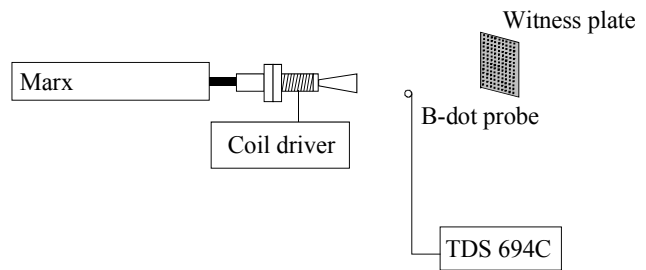


Figure 13. Experimental arrangement for the BWO System.

The BWO was designed to deliver a 35 GHz signal within a 3 – 4 ns envelope. As shown in Figure 14, the system appears to deliver a 20 ns window of microwave energy that was approximated to be 30 MW in peak power. As illustrated in the photograph of Figure 15, the BWO delivered a  $TM_{01}$  mode.

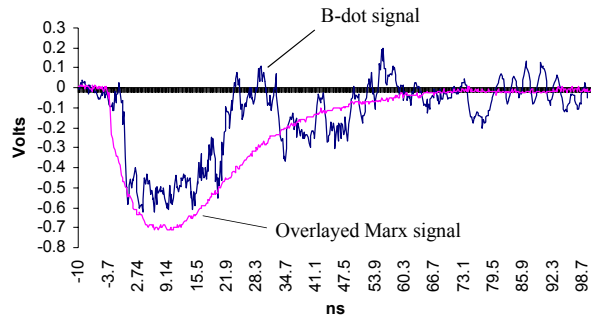


Figure 14. Results from the BWO testing.

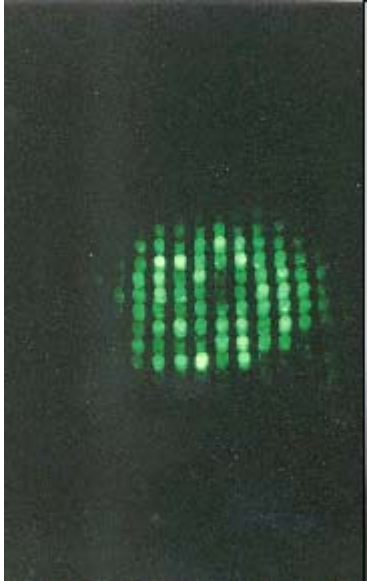


Figure 15. Fluorescent plate, witnessing the BWO radiation.

#### D. The Gatling Marx Generator System

The Gatling Marx Generator system is partially based on the Injection Wave Generator<sup>7</sup> system in that multiple, independent sources inject energy onto a common transmission line. In the case of the Gatling system, the independent sources are Marx generators, each capable of injecting hundreds of kV onto the common transmission line. Each generator is isolated from the line with a magnetic switch. This system offers flexibility of variable voltage levels, variable voltage polarity and variable temporal spacing between the high voltage pulses.

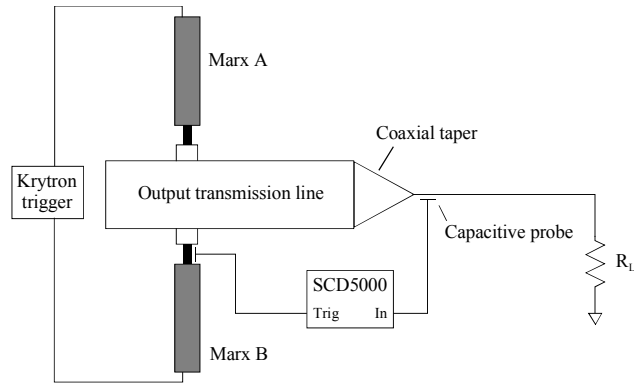


Figure 16. The experimental Gatling Marx generator system.

The demonstration system is shown in Figure 16. The three Marx generators are orthogonally connected to the common transmission line, and for the purpose of demonstration, the generators have a common trigger system. A capacitive voltage probe is placed at the trigger input of Marx A, and a current-viewing resistor is placed at the output of the common transmission line. Each of the generators is designed to deliver a 140 kV pulse with sub-nanosecond risetimes.

As illustrated in Figure 17, the output of the current-viewing resistor demonstrates the system's ability to generate three distinct high voltage pulses, each having an amplitude in excess of 125 kV.

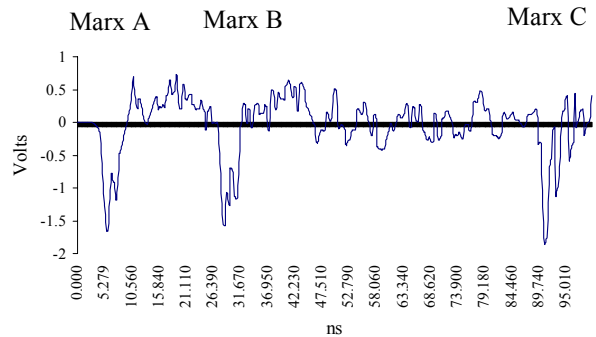


Figure 17. An example output waveform from the Gatling Marx Generator system.

The Gatling Marx system was connected to the TEM horn used in earlier in this discussion. The three distinct radiated pulses are evident in Figure 18. Precautions were taken to ensure that the antenna did not break down during the first pulse so that the later pulses would be radiated.

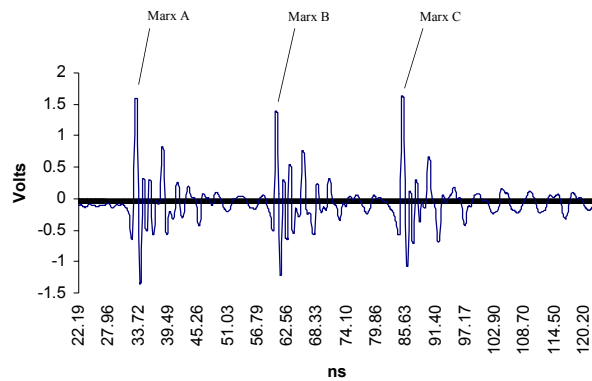


Figure 18. A radiated signal from the Gatling Marx Generator system.

## VI. CONCLUSION

This paper presented two compact Marx generators and associated applications. The first generator was designed for impulse applications and is capable of delivering voltages in excess of 300 kV with extremely fast risetimes. Temporal jitter reduction techniques were presented, with an experimental demonstration of 114 ps rms resulting. The generator was also used to generate microwave energy in the form of an Ultra Wideband signal. Finally, this generator was used as the source of a novel Gatling Marx generator system, which illustrated the ability to launch multiple pulses from unique sources onto a common transmission line.

The second generator was designed for driving the Backward Wave Oscillator. The system successfully produced a 35 GHz signal in a 20 ns window in the  $TM_{01}$  mode.

Future work with these generators will concentrate on increasing the output power, as well as increasing the repetition rate. Future antenna work will aim at maximizing the effective radiated power.

## References

1. W.C. Nunnally, The University of Missouri-Columbia, Columbia, Missouri, 65211
2. L. Altgilbers, U.S. Army Space and Missile Defense Command, Huntsville, Alabama , 35807-3801
3. M. Kristiansen, Texas Tech University, Lubbock, Texas 79410.
4. U.S. Army Contract Number DASG60-99-C-0079.
5. U.S. Army Contract Number DASG60-99-M-0051.
6. G. Schaefer, Gas Discharge Closing Switches, Plenum Press, New York, 1990.
7. J.R. Mayes, Dissertation, The University of Missouri-Columbia, 1998.